On energy storage of Lu2O3:Tb,M (M=Hf, Ti, Nb) sintered ceramics: Glow curves, dose-response dependence, radiation hardness and self-dose effect

Kulesza, Dagmara; Bos, Adrie J.J.; Zych, Eugeniusz

DOI
10.1016/j.jallcom.2018.07.360

Publication date
2018

Document Version
Accepted author manuscript

Published in
Journal of Alloys and Compounds

On Energy Storage of Lu_2O_3:Tb,M (M=Hf, Ti, Nb) Sintered Ceramics: Glow Curves, Dose-Response Dependence, Radiation Damage and Self-Dose Effect

Dagmara Kulesza*[,1], Adrie J. J. Bos[2], and Eugeniusz Zych[1]

[1]*Faculty of Chemistry, University of Wrocław*
14 F. Joliot-Curie Street, 50-383 Wrocław, Poland

[2]*Faculty of Applied Sciences, Delft University of Technology*
Mekelweg 15, NL 2629 JB Delft, The Netherlands

* corresponding author: dagmara.kulesza@chem.uni.wroc.pl

Abstract

Thermoluminescent properties and energy storage characteristics of Lu_2O_3:Tb,M (M=Hf, Ti, Nb) sintered ceramics induced by ionizing radiation are presented and discussed. Dose-response dependence, radiation hardness and fading were studied. A linearity of the former exceeding seven orders of magnitude was confirmed for Lu_2O_3:Tb,Hf and Lu_2O_3:Tb,Nb ceramics. Lu_2O_3:Tb,Hf showed the best TL performance and also its fading was the lowest reaching 15 % over 7 hours and showed tendency to saturate. During the same period of time the Lu_2O_3:Tb,Ti, despite having TL at higher temperatures, lost about 25 % of the stored energy and the TL signal of Lu_2O_3:Tb,Nb faded by almost 40 % over 7 hours. First order TL kinetics was confirmed for all three compositions. A self-dose effect in Lu_2O_3:Tb,Hf due to a natural content of the radioactive isotope (2.6 %) was proved to be important for long-time reading of low doses.

Introduction

Energy storage and persistent luminescence phosphors are very much needed for a whole variety of known and emerging applications/technologies. These varies from simple gadgets based on persistent (glow-in-the dark) phosphors decorations, dials, pigments and plastics through emergency signalization, safety displays and clothing, road marks to dosimetry, background-free medical- and bio-imaging, diagnostics and therapy, thermometry, and environmental control [1][2][3][4][5][6][7]. The various uses share some common requirements [8][9][10] – high sensitivity, wide linearity of dose-response dependence, low fading (storage phosphors), good match of the emission wavelength with detector sensitivity, mechanical strength, chemical inertness and non-hygroscopicity. High sensitivity is especially important for use in personal and medical dosimetry, as well as in environmental radiation monitoring [8]. Currently the most sensitive TL materials are Al_2O_3:C, CaF_2:Mn and LiF:Mg,Cu,P able to detect even 0.05 μGy, 0.1 μGy and 1 μGy, respectively [8][11][12][13][14]. These crucial parameters for the title compositions will be reported in this paper. Large range of linear dose-response dependence allows for accurate reading of greatly different doses. Main dosimeters fulfilling this requirements are CaF_2:Mn (TLD-400), with good linearity over ~1 μGy-100 Gy and $Li_2B_4O_7$:Mn (TLD-800) with the useful dose range of 1 mGy-10^5 Gy.

Typically the requirement of low dependence of the absorption coefficient to the energy of incoming particles - which translates to low dependence of the TL response to the radiation energy – is also of great importance for dosimetric materials used in most present applications. This makes the dosimeter response to the ionizing radiation similar to the response of tissues [15]. Therefore, the effective Z-number, Z_{eff}, of the dosimeter should be possibly close to the Z_{eff}-number of water (Z_{eff} = 7.4), the main constituent of human body [16]. This condition explains the broad use of LiF-based dosimeters for which the Z_{eff} = 8.2. Even some sensitivity of LiF to humid/moisture is tolerated for advantages it offers.

The requirement of tissue equivalence appears much less crucial when it comes to high-dose dosimetry important in monitoring of such processes as sterilization, disinfection, modification of materials properties by means of ionizing radiation, controlling defects in large machines parts [9][10]. High-doses monitoring is also needed to inspect radiation in nuclear power stations and wherever a spent nuclear fuel is stored. High-doses reading raises new demands the dosimeters should fulfil, however. First, the already mentioned linearity of the response has to extend to the region of the expected (high) doses to be monitored. Another critical condition in such applications is related to the dosimeters radiation hardness. Some materials show low radiation hardness and after exposure to high doses they lose their storage properties. For example, LiF:Mg,Cu,P detector can be exposed to high doses only ones as there is no technological procedure known to restore its original storage properties afterwards. In contrary, the TLD-500 dosimeter (Al_2O_3:C) after exposure to high doses may recover its original storage properties by a heat-treatment at 900 °C for 1 hour [9][17]. Obviously, it would be most desirable – for convenience and cost efficacy - to have the dosimeter ready for a next run just after its TL reading. This parameter is also a subject of the studies of the title compositions and is reported in this paper.

It is noteworthy that a combined use of both low-Z and high-Z dosimeters would allow to determine the incoming radiation quality (energy) quickly and reliably – a purpose typically still not addressed by dosimetric examinations at all [18][19][20]. In principle, for that function, a higher difference of the effective Z_{eff}-numbers of the combined dosimeters should allow for a better assessment of the radiation quality. Thus, nowadays, when the spectrum of dosimeters' applications broadens, also high-density, high-Z number materials are not excluded from the field of dosimetry. With this in mind investigation of Lu_2O_3-based storage phosphors appears important not only from the point of view of fundamental research.

We have previously reported on thermoluminescent (TL) properties of a series of Lu_2O_3:Tb,M (M=Ca/Sr/Ba, Hf, Ti, Nb) sintered ceramics [21][22][23][16]. Their thermoluminescence characteristics were largely gathered following irradiation of the materials with short-wavelength UV radiation (250-320 nm). However - especially in the case of as heavy compositions as Lu_2O_3 (density ρ=9.4 g/cm^3 [24][25], and Z_{eff}=67.3), whose conceivable applications are related to digital radiography and imaging at first and possibly, as we stated above, to high-dose dosimetry or radiation quality assessment - much more interesting is to identify and comprehend their characteristics resulting from exposure to ionizing radiation.

A technological process for making an array of densely-packed needle-like structure of CsBr:Eu^{2+} storage phosphor allowed to greatly increase the spatial resolution of images in computed radiography [26][27][28]. Analogously to CsBr, Marton *et al*. [29] developed a procedure to produce microcolumnar Lu_2O_3:Eu scintillator and showed that it offers greatly improved image resolution due to restrained light smudging. There is no reason to doubt that making such columnar structures of Lu_2O_3:Tb,M storage phosphors would also be manageable

making it attractive for 2D imaging, like computed radiography [26]. All of that encouraged us to acquire detailed data on energy storage properties of the three Lu_2O_3:Tb,M (M=Hf, Ti, Nb) storage phosphors upon exposure to ionizing radiation. In this paper we concentrate on the dose-response dependence, radiation hardness, fading and self-dose effect due to the radioactive ^{176}Lu present for 2.6 % in the natural lutetium.

Materials and methods

Fabrication procedure of the materials was presented in detail previously [16]. In short, powders prepared by Pechini method were cold-pressed and sintered at 1700 °C for 5 hours in vacuum (Tb,Hf), air (Tb,Nb) or forming gas (Tb,Ti). The different atmospheres were applied as they were previously proved to give materials of better performance, though the effect of the atmosphere did not exceed a factor of 2-3 in TL efficiency for any of them. The produced pellets were ground and polished before measurements to remove the thermally etched surface layer.

Crystallographic purity of the samples was checked by XRD technique using a Bruker D8 Advance diffractometer using Cu K_α radiation. The TL measurements were performed with a Risø TL/OSL reader model DA-15 and a controller model DA-20 with heating rate of 5 °C/s. The TL emission spectra vs. temperature (λT-contour plots) were measured after the materials were exposed to 1.3 kGy from an external ^{60}Co source. Simulation of the TL glow curves were performed assuming first-order kinetics.

The fading of the TL glow curves was measured with various delay time after the samples irradiation with ^{90}Sr/^{90}Y β-source with a dose rate of 0.7 mGy/s. Exposition time to β particles was different for each material, 4 s for (Tb,Hf) doped sample, 60 s for (Tb,Nb) and 100 s in case of (Tb,Ti) ceramics. A BG39 filter was used to block infrared (IR) and red radiation at higher temperatures to reach PM tube. The dose-response dependence was measured over wide dose range (1 μGy to 2 kGy) for all three compositions. To achieve this, sources with different dose rates were utilized. For the low dose range a ^{90}Sr/^{90}Y source with a dose rate of 0.5 μGy/s was used. In this dose range the PMT was placed as close as possible to the sample. In the mGy dose range a ^{90}Sr/^{90}Y source with a dose rate of 0.7 mGy/s was used while the distance between the sample and PMT was increased. For doses in the Gy range a diaphragm with a pin hole of 1.1 mm diameter in front of the PM tube was used in order to prevent saturation of the detector. For the dose in the kGy range a ^{60}Co source with a dose rate of 0.36 Gy/s was applied. Samples exposed to these high doses were read out with a diaphragm with a pin hole of 0.5 mm and a grey filter with a 1% transmission.

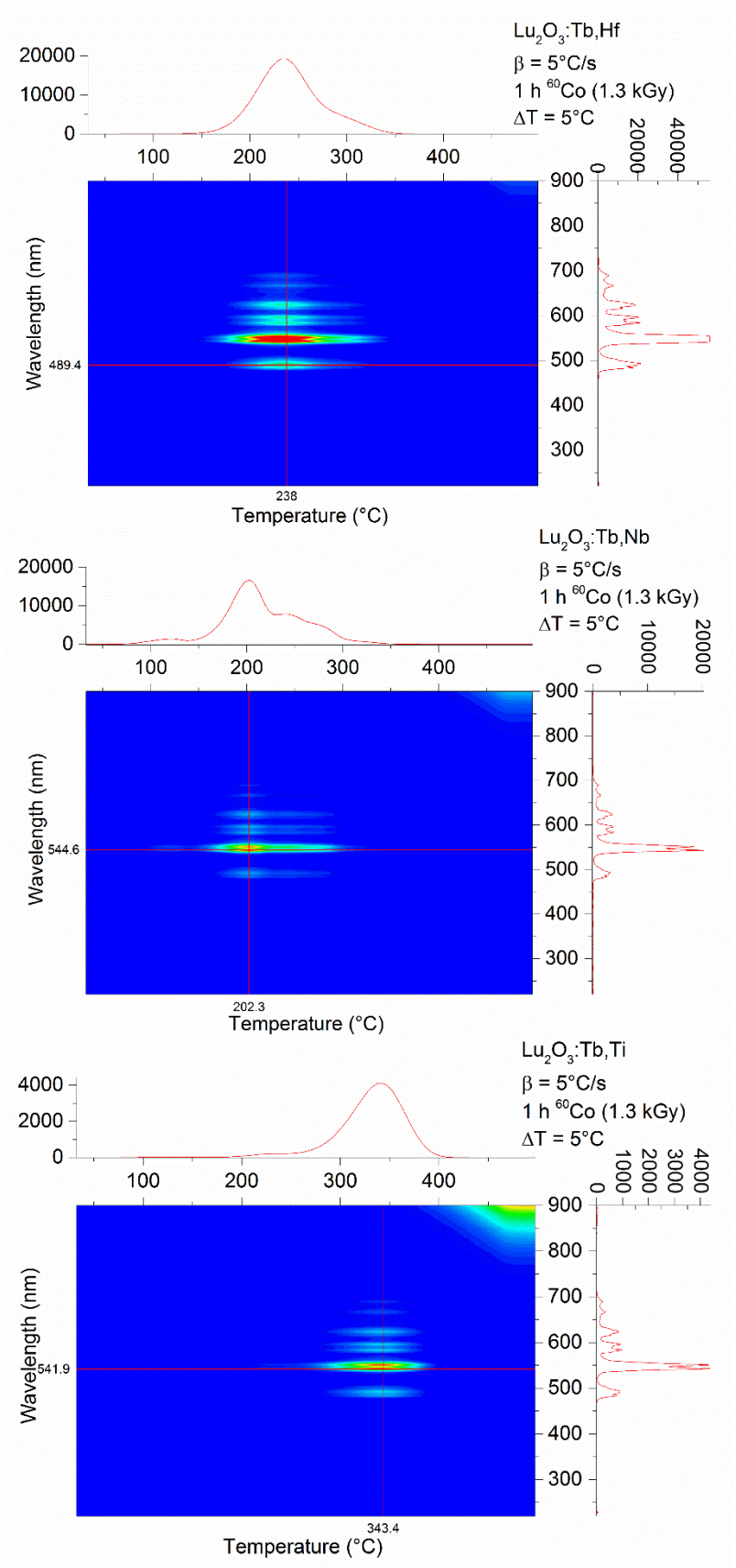

Figure 1. Thermoluminescence as function of temperature and wavelength for Lu_2O_3 samples doped with (Tb,Hf) top, (Tb,Nb) middle and (Tb,Ti) bottom.

Results and discussion

Thermoluminescence. Fig. 1 displays temperature- and wavelength-resolved thermoluminescent contour graphs for all the three Lu_2O_3:Tb,M (M=Hf,Nb,Ti) ceramics recorded after ^{60}Co γ-ray irradiation. Independently on the co-dopant exclusively the Tb^{3+} ions serve as recombination centers producing its characteristic green luminescence with the most prominent component around 545 nm resulting from the $^5D_4 \rightarrow {}^7F_5$ transition. Hf, Nb and Ti co-dopant strongly determine the trapping sites depths and efficiency of the TL. As a result the most intensive TL glow peaks can be observed at about 240, 200 and 340 °C (with β = 5 ˚C/s) for Hf, Nb and Ti co-doping, respectively. In Fig. 2a the measured glow curves for the three compositions are presented. Attempts were made to determine the trap depths of the main glow peaks by glow curve fitting using a first-order glow peak according to Randall and Wilkins [30][31] after correcting the curves for thermal quenching (Fig.2b). It appears not possible to find good fit parameters values consistent at different doses and different heating rates. A rough indication of the trap depth was made assuming a value of the frequency factor *s* = 1.7×10^{13} s^{-1}. This value is estimated based on the reported fundamental vibrations of the Lu_2O_3 host-lattice of 580 cm^{-1} [32]. With this values of *s* and the measured temperature at glow peak maximum we derived the following trap depths: 1.33 eV (Nb), 1.44 eV (Hf) and 1.76 eV (Ti). It is clear from Fig. 2b that the mechanism of main TL glow in each in the materials is more complex than the One Trap One Recombination centre (OTOR) model from which Randall and Wilkins derived their equation. Nevertheless, the data in Fig. 2 prove that the traps giving rise to the main TL glow peaks are quite deep and they presumably should be capable of storing energy for long time with negligible fading, at most. We shall see later that the reality is more complex.

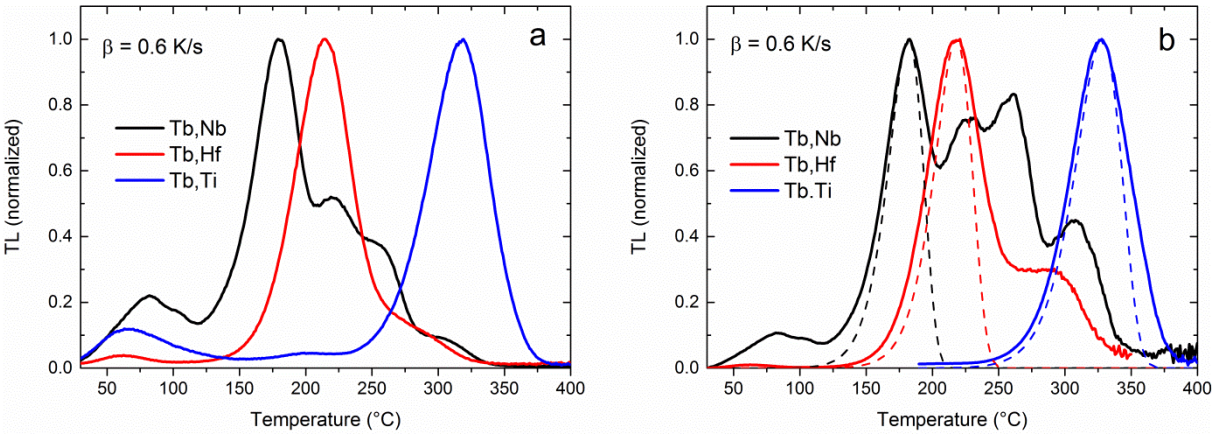

Figure 2. Glow curves of Lu_2O_3:Tb,M as measured (a) and corrected for thermal quenching (b). The dotted lines are simulated glow curves based on the Randall-Wilkins equation with the estimated trap depths and frequency factor (see text).

Dose response

The dose dependence of TL is of prime importance in case of potential practical usability of dosimeters and storage phosphors [33]. To reliably read the relevant information the absorbed dose should correspond to the measured thermoluminescence intensity. A linear dose-response dependence over possibly widest range of doses is desirable.

Fig. 3 shows a comparison of the dose-response dependence for all the three members of the Lu_2O_3:Tb,M series. It is well seen that the (Tb,Hf) doped sample is 20 times more sensitive than the (Tb,Nb) doped material and even 80 times than (Tb,Ti) sample. This however, does not necessary mean that the latter composition is least efficient in energy storage. Since its TL occurs at highest temperatures it suffers the most from the thermal quenching as reported previously [16]. As might be expected then, due to the lowest TL signal, out of the three compositions the (Tb,Ti) ceramic storage phosphor is the least sensitive for the lowest doses. Its low dose detection limit is 0.1 mGy. Above this level the dose-response dependence for the (Tb,Ti) ceramics is practically linear up to ~ 500-600 Gy. Exact analysis, see Fig. 4, reveals that before saturation a small supralinearity occurs, while the (Tb,Hf) ceramics does not show such an effect. For the Lu_2O_3:Tb,Hf and the Lu_2O_3:Tb,Nb below 10 µGy the response is not linear, though (especially for the (Tb,Hf) sample) it slowly increases with the dose. This means that the sensitivity of these two ceramics is about two orders of magnitude lower compared to Al_2O_3:C [11]. However, both Lu_2O_3:Tb,Hf and Lu_2O_3:Tb,Nb response linearly over more than seven orders of magnitude starting from ~10 µGy and lasting to ~100-200 Gy. At yet higher doses both materials respond supralinearly and finally saturate above 1 kGy, presumably due to complete filling of the available traps, see Figs. 3 and 4.

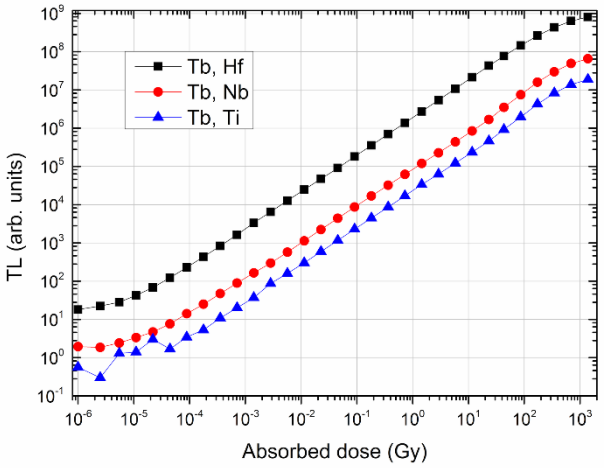

Figure. 3. Dose response curves of Lu_2O_3:Tb,M (M = Hf ,Nb, Ti) measured after exposure with sources with different dose rates.

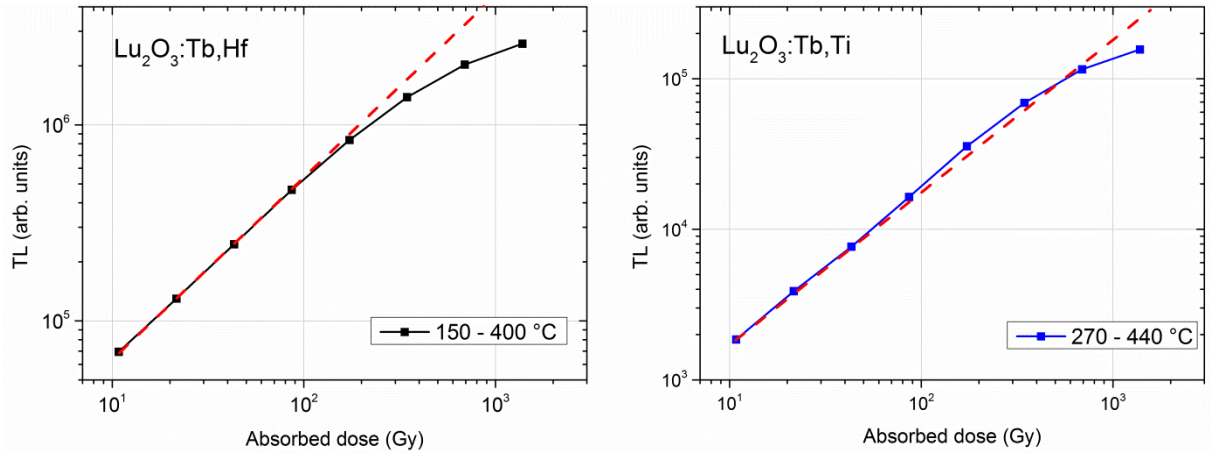

Figure 4. Dose response curves of Lu_2O_3:Tb,M (M = Hf, Ti) in the high dose range (upper right part of Fig. 3). The (Tb,Ti) doped sample (on the right) shows some supralinearity.

Consequently, for the (Tb,Hf) and (Tb,Nb) ceramics, their useful range extent over ~10 µGy – ~200 Gy, covering the areas exploited in environmental, personal, radiotherapy and radiation processing dosimetry. What is important, neither the shape of the glow curves nor the emission spectra change in the whole wide dose range for either of the compositions (Fig. 5 presents relevant data for the Tb,Hf ceramics). Simultaneously, the assumed first-order kinetics of the ceramics TLs is justified. Thus, the reading procedure is perfectly the same independently on the read dose.

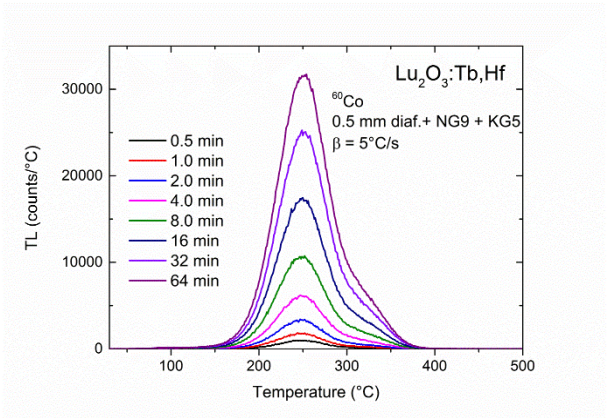

Figure 5. TL glow curves of Lu_2O_3:Tb,Hf after different doses (1 min= 21.6 Gy).

Of equal importance, after a dose in the kGy range, the materials could be used again to measure a dose in the 10 µGy range, so no radiation damage could be observed after such a high dose. Consequently, after TL reading the materials do not require any additional treatment to sensitize them. Such stability of keeping the luminescent and dosimetric properties stable under high exposure doses characterizes only radiation resistance materials. Among them we find $YAlO_3$:Mn (Z_{eff} = 31.4), a good candidate for middle- and high- dose dosimetry particularly where tissue equivalence is not an issue [34][35].

Self dose

A crucial factor for detectors used in the low dose range is the background signal. The background can be seriously increased by a self-dose, the signal produced by the radioactive content of the thermoluminescent material. In case of detectors used to measure long time exposure effects or very low dose detection the self-irradiation phenomenon should be taken into account. Pashchenko et al. trying to determine fading effect of TL in KCl:Eu^{2+} crystals found that self-dose due to radioactive ^{40}K needs to be considered [36][37]. The same radionuclide contributes to high self-dose (~1.5 µGy/h) in $KMgF_3$:Ce, an ultrasensitive OSL material whose low dose detection limit was found to be one order of magnitude greater than Al_2O_3 [38][39]. The self-irradiation occurs obviously for entire series of Lu_2O_3:Tb,M samples, but quantitative results we present for (Tb,Hf)-doped material.

Natural lutetium contains an radio-active isotope, ^{176}Lu, abundance of 2.6%, with a very long half-life, $(3.64\pm0.07)\times10^{10}$ y giving rise to a specific activity of 52 Bq/g. The decay is for 100% via beta particle emission. Most energy of the emitted beta particle (E_{max} = 593 keV, E_{ave} = 182 keV) will be absorbed in the sample. The radioisotope decays to ^{176}Hf in an exited state. De-excitation to the ground state will produce some gamma quanta (307 keV, 202 keV and 88 keV). The element change will also produce some characteristic X-rays of which the $K_{\alpha,\beta}$ of 54 keV is the most important. The gamma- and X-rays will partly be absorbed in the sample (quite effectively due to lutetia high density). The energy absorption of all mentioned radiation types will contribute to a TL signal, a so-called self-dose. For Lu_2O_3:Tb,Hf an estimation of the self-dose rate based on the assumption that all produced beta particles and gamma and X-rays are completely absorbed gives 0,2 mGy/day. This is quite high compared to the dose rate of natural sources (cosmic/terrestrial) of ≈ 1 µGy/day (rule of thumb for the Netherlands).

To measure the self-dose the (Tb,Hf) doped sample was read out and stored for 101.3 h in darkness. The signal after that storage time is shown in Fig. 6. The signal corresponds with a dose of 1.3 mGy which means 0,3 mGy/day, slightly higher than estimated but lower than the self-dose from ^{40}K in $KMgF_3$:Tl (0,8 mGy/dag, [40]) and ^{87}Rb in $RbMgF_3$:Eu (1.0 mGy/day, [41]). Simultaneously we measured the storage dose with Al_2O_3:C, a reference TL material, and found 5,6 µGy, so 1.3 µGy/day. This value agrees very well with what you expect from natural sources. Anyway, the self-dose in Lu_2O_3 cannot be neglected.

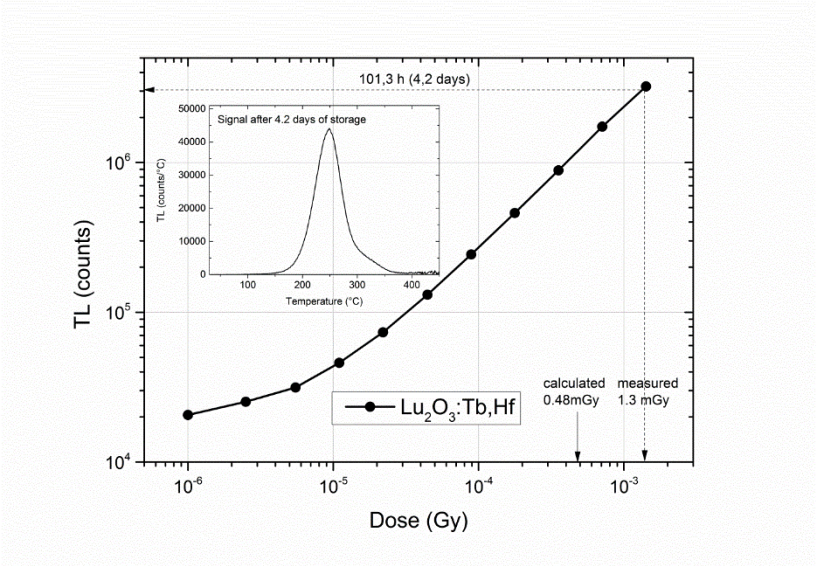

Figure 6. Dose response curve of Lu_2O_3:Tb,Hf in the low dose range (lower part of the Fig. 3).

Short-term fading

The next feature of paramount importance in group of dosimeters and energy storage materials is their ability to accumulate of the acquired energy until readout. Although some data were presented for (Tb,Hf) doped material after UV exposition in a previous paper [23], here we show precise results for entire group within first few hours after excitation with β radiation. Fig. 7 presents the fading behavior for the three Lu_2O_3:Tb,M samples. The integrated area of the TL glow band around the main peak as a function of the delay time provides the so-called fading rate curves shown on the right side of the figures. Some fading of TL is observed for all samples but the extents differ significantly. The shallow traps (low temperature peaks) fades almost totally, but the leak of trapped charge is also seen from high-temperature traps. For (Tb,Ti) doped sample the fading rates for the high-temperature part of TL curve in first ~7 hours is almost ~25% and seems to be stable at this point. For (Tb,Nb) the fading within the first 7 hours is close to 40% and the energy still tends to leak from the traps. For the (Tb,Hf) material TL intensity drop is about 15% and seems to show a tendency to stabilize around this value.

Taking into account the location of the main peak for each co-dopant and a rational assumption that deeper trap should reduce the probability of charge leakage the results differ from the expectations. There is no relation between the degree of fading and positions of glow peak maxima. This may be explained by spatially correlated trapping and recombination centers such that there is a possibility of a centre-to-centre recombination, a transition in which the conduction band does not participate and does not serve as a pathway for the carriers escaping their traps. The phenomenon of centre-to-centre recombination is not a rare situation and was concluded for example in $YPO_4:Ce^{3+},Sm^{3+}$ leading to an unexpectedly high fading rate of its high-temperature TL peak [42].

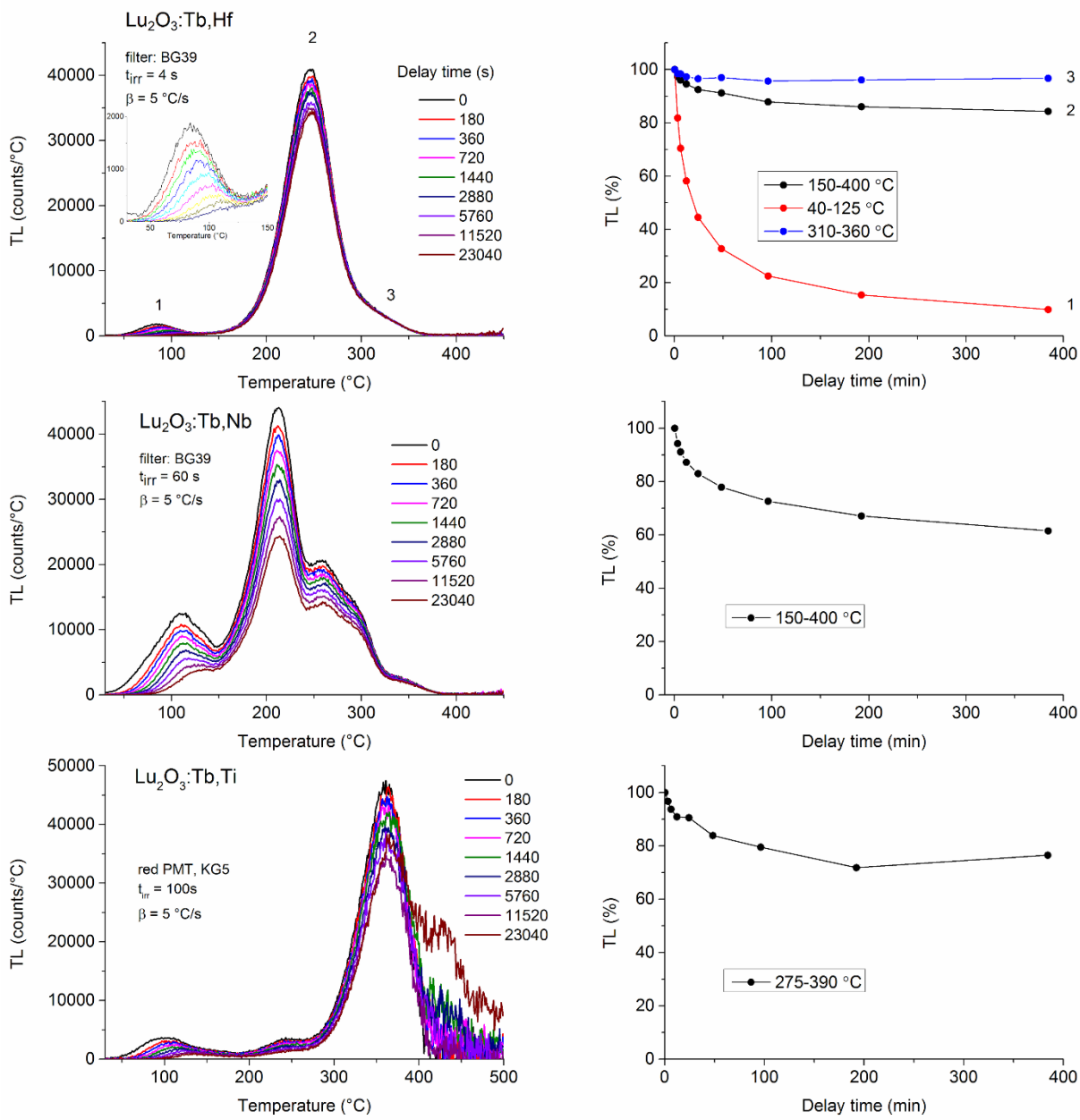

Figure 7. Fading behavior of TL in Lu_2O_3:Tb,M (M= Hf, Nb, Ti) samples. The delay time is the duration between the end of the irradiation and the start of the readout. On the right the fading rate curves for a given co-doped materials are presented.

Conclusions

The thermoluminescence characterization and energy storage properties were performed for Lu_2O_3:Tb,M (M = Hf, Nb, Ti) materials upon ionizing radiation. The thermoluminescence measurements show that in all samples the Tb^{3+} serves as a recombination center, while the M co-dopants do not produce any emission. The co-dopants strongly determine the amount of charge that is trapped during exposure to ionizing radiation. Of all investigated Lu_2O_3 samples the Hf co-doped material gives the highest TL signal per unit dose. The dose response is linear for each material over a wide dose range. For the Lu_2O_3:Tb,Hf and Lu_2O_3:Tb,Nb

samples over seven orders of magnitude. The radiation hardness is remarkably high, as after a dose of 1 kGy no change in response to small doses was observed. All investigated samples show some fading. There is no relation between the fading rate and the temperature of the glow peak maximum. Because of the presence of ^{176}Lu natural radio-active isotope the samples show self-dose effect, which for Lu_2O_3:Tb,Hf was found to reach 0.3 mGy/day.

Acknowledgements

The authors gratefully acknowledge financial support by the Polish National Science Centre (NCN) under the grant #UMO-2014/13/B/ST5/01535.

References

[1] Y. Li, M. Gecevicius, J. Qiu, Long persistent phosphors—from fundamentals to applications, Chem. Soc. Rev. 45 (2016) 2090–2136. doi:10.1039/C5CS00582E.

[2] H. Terraschke, C. Wickleder, UV, Blue, Green, Yellow, Red, and Small: Newest Developments on Eu2+-Doped Nanophosphors, Chem. Rev. 115 (2015) 11352–11378. doi:10.1021/acs.chemrev.5b00223.

[3] V. Lojpur, S. Ćulubrk, M. Medić, M. Dramicanin, Luminescence thermometry with Eu3+ doped GdAlO3, J. Lumin. 170 (2016) 467–471. doi:10.1016/j.jlumin.2015.06.032.

[4] D. Jaque, C. Richard, B. Viana, K. Soga, X. Liu, J.G. Solé, Inorganic nanoparticles for optical bioimaging, Adv. Opt. Photon. 8 (2016) 1–103. doi:10.1364/AOP.8.000001.

[5] R. Weissleder, M.J. Pittet, Imaging in the era of molecular oncology., Nature. 452 (2008) 580–9. doi:10.1038/nature06917.

[6] B. Viana, S.K. Sharma, D. Gourier, T. Maldiney, E. Teston, D. Scherman, C. Richard, Long term in vivo imaging with Cr3+ doped spinel nanoparticles exhibiting persistent luminescence, J. Lumin. 170 (2016) 879–887. doi:10.1016/j.jlumin.2015.09.014.

[7] G. Li, Y. Wang, W. Zeng, W. Chen, S. Han, H. Guo, J. Liu, Effects of Nd 3 + co-doping on the long lasting phosphorescence and optically stimulated luminescence properties of green emitting, Mater. Res. Bull. 84 (2016) 1–6. doi:10.1016/j.materresbull.2016.07.020.

[8] V. Kortov, Materials for thermoluminescent dosimetry: Current status and future trends, Radiat. Meas. 42 (2007) 576–581. doi:10.1016/j.radmeas.2007.02.067.

[9] V. Kortov, Modern trends and development in high-dose luminescent measurements, J. Phys. Conf. Ser. 552 (2014) 12039. doi:10.1088/1742-6596/552/1/012039.

[10] S.W.S. McKeever, M. Moscovitch, P.D. Townsend, Thermoluminescence dosimetry materials: properties and uses, Nuclear Technology Pub., 1995. https://books.google.pl/books?id=wBtRAAAAMAAJ.

[11] M.S. Akselrod, V.S. Kortov, D.J. Kravetsky, V.I. Gotlib, Highly Sensitive Thermoluminescent Anion-Defective Alpha-Al203:C Single Crystal Detectors, Radiat.

Prot. Dosimetry. 32 (1990) 15. doi:10.1093/oxfordjournals.rpd.a080715.

[12] K.J. Velbeck, L.Z. Luo, M.J. Ramlo, J.E. Rotunda, The dose-response of Harshaw TLD-700H., Radiat. Prot. Dosimetry. 119 (2006) 255–258. doi:10.1093/rpd/nci526.

[13] T. Nakajima, Y. Murayama, T. Matsuzawa, A. Koyano, Development of a new highly sensitive LiF thermoluminescence dosimeter and its applications, Nucl. Instruments Methods. 157 (1978) 155–162. doi:http://dx.doi.org/10.1016/0029-554X(78)90601-8.

[14] A.J.J. Bos, High sensitivity thermoluminescence dosimetry, Nucl. Instruments Methods Phys. Res. Sect. B Beam Interact. with Mater. Atoms. 184 (2001) 3–28. doi:10.1016/S0168-583X(01)00717-0.

[15] M. Kurudirek, Effective atomic numbers, water and tissue equivalence properties of human tissues, tissue equivalents and dosimetric materials for total electron interaction in the energy region 10keV-1GeV, Appl. Radiat. Isot. 94 (2014) 1–7. doi:10.1016/j.apradiso.2014.07.002.

[16] D. Kulesza, P. Bolek, A.J.J. Bos, E. Zych, Lu2O3-based storage phosphors. An (in)harmonious family, Coord. Chem. Rev. 325 (2016) 29-40.

[17] V.S. Kortov, S. V. Zvonarev, V.A. Pustovarov, A.I. Slesarev, Features of thermoluminescence in anion-defective alumina single crystals after highdose irradiation, Radiat. Meas. 61 (2014) 74–77. doi:10.1016/j.radmeas.2013.12.010.

[18] Z. Xia, J. Zhuang, L. Liao, Novel Red-Emitting Ba 2 Tb (BO 3) 2 Cl : Eu Phosphor with E ffi cient Energy Transfer for Potential Application in White Light-Emitting Diodes, (2012).

[19] Y. Zhydachevskii, A. Morgun, S. Dubinski, Y. Yu, M. Glowacki, S. Ubizskii, V. Chumak, M. Berkowski, A. Suchocki, Energy response of the TL detectors based on YAlO3: Mn crystals, Radiat. Meas. 90 (2015) 262–264. doi:10.1016/j.radmeas.2015.12.001.

[20] Z. Spurny, Some New Materials for TLD, Nucl. Instruments Methods. 175 (1980) 71–73.

[21] D. Kulesza, J. Trojan-Piegza, E. Zych, Lu2O3:Tb,Hf storage phosphor, in: Radiat. Meas., 2010: pp. 490–492.

[22] D. Kulesza, A. Wiatrowska, J. Trojan-Piegza, T. Felbeck, R. Geduhn, P. Motzek, E. Zych, U. Kynast, The bright side of defects: Chemistry and physics of persistent and storage phosphors, in: J. Lumin., 2013: pp. 51–56.

[23] D. Kulesza, E. Zych, Managing the Properties of Lu 2 O 3 :Tb,Hf Storage Phosphor by Means of Fabrication Conditions, J. Phys. Chem. C. 117 (2013) 26921–26928. doi:10.1021/jp410313w.

[24] M. Guzik, J. Pejchal, A. Yoshikawa, A. Ito, T. Goto, M. Siczek, T. Lis, G. Boulon, Structural Investigations of Lu2O3 as Single Crystal and Polycrystalline Transparent Ceramic, Cryst. Growth Des. 14 (2014) 3327–3334. doi:10.1021/cg500225v.

[25] J. Zeler, L. Jerzykiewicz, E. Zych, Flux-Aided Synthesis of Lu2O3 and Lu2O3:Eu—Single Crystal Structure, Morphology Control and Radioluminescence Efficiency, Materials (Basel). 7 (2014) 7059–7072. doi:10.3390/ma7107059.

[26] P. Leblans, D. Vandenbroucke, P. Willems, Storage phosphors for medical imaging, Materials (Basel). 4 (2011) 1034–1086. doi:10.3390/ma4061034.

[27] B. Schmitt, M. Fuchs, E. Hell, W. Kn??pfer, P. Hackenschmied, A. Winnacker, Structured alkali halides for medical applications, Nucl. Instruments Methods Phys. Res. Sect. B Beam Interact. with Mater. Atoms. 191 (2002) 800–804. doi:10.1016/S0168-583X(02)00656-0.

[28] N.M. Winch, A. Edgar, X-ray imaging using digital cameras, 8313 (2012) 83135E. doi:10.1117/12.911146.

[29] Z. Marton, H.B. Bhandari, C. Brecher, S.R. Miller, B. Singh, V. V Nagarkar, High efficiency microcolumnar Lu2O3:Eu scintillator thin film for hard X-ray microtomography, J. Phys. Conf. Ser. 425 (2013) 62016. doi:10.1088/1742-6596/425/6/062016.

[30] J.T. Randall, M.H.F. Wilkins, Phosphorescence and Electron Traps. I. The Study of Trap Distributions, Proc. R. Soc. London. Ser. A. Math. Phys. Sci. 184 (1945) 365 LP-389. http://rspa.royalsocietypublishing.org/content/184/999/365.abstract.

[31] J.T. Randall, M.H.F. Wilkins, Phosphorescence and Electron Traps. II. The Interpretation of Long-Period Phosphorescence, Proc. R. Soc. London. Ser. A. Math. Phys. Sci. 184 (1945) 390 LP-407. http://rspa.royalsocietypublishing.org/content/184/999/390.abstract.

[32] E. Zych, A. Meijerink, C.D.M. Doneg, Quantum efficiency of europium emission from nanocrystalline powders of Lu 2 O 3 : Eu, J. Phys. Condens. Matter. 15 (2003) 5145–5155. doi:Pii S0953-8984(03)62446-X.

[33] R. Chen, V. Pagonis, Thermally and Optically Stimulated Luminescence: A Simulation Approach, John Wiley & Sons, 2011. https://books.google.pl/books?id=Bm_kd7sWXwQC.

[34] Y. Zhydachevskii, A. Suchocki, M. Berkowski, P. Bilski, S. Warchol, Characterization of YAlO3:Mn2+ thermoluminescent detectors, Radiat. Meas. 45 (2010) 516–518. doi:http://dx.doi.org/10.1016/j.radmeas.2009.12.035.

[35] Y. Zhydachevskii, A. Suchocki, M. Berkowski, Y. Zakharko, Optically stimulated luminescence of for radiation dosimetry, Radiat. Meas. 42 (2007) 625–627. doi:10.1016/j.radmeas.2007.01.054.

[36] L.P. Pashchenko, R.P. Salas, R. Aceves, M. Barboza-Flores, Fading and self-irradiation of potassium halide thermoluminescence dosimeters, Appl. Phys. Lett. 66 (1995) 1–3. doi:10.1063/1.113624.

[37] L.P. Pashchenko, R. Pérez Salas, R. Aceves, M. Barboza-Flores, A simple calibration method for potassium halide thermoluminescence dosimeters, Appl. Phys. Lett. 67 (1995). doi:10.1063/1.114893.

[38] N.J.M. Le Masson, A.J.J. Bos, C.W.E. Va Eijk, C. Furetta, J.P. Chaminade, Y.S. Horowitz, L. Oster, Optically and thermally stimulated luminescence of KMgF3:Ce3+ and NaMgF3:Ce3+, Radiat. Prot. Dosimetry. 100 (2002) 229–234. doi:10.1093/oxfordjournals.rpd.a005853.

[39] N.J.M. Le Masson, A.J.J. Bos, A.J.M. Winkelman, C.W.E. van Eijk, Optically stimulated luminescence in KMgF/sub 3/:Ce/sup 3+/ comparison of dosimetric characteristics with Al/sub 2/O/sub 3/:C, IEEE Trans. Nucl. Sci. 48 (2001) 1143–1147. doi:10.1109/23.958739.

[40] P.R. González, C. Furetta, J. Azorín, T. Rivera, G. Kitis, F. Sepúlveda, C. Sanipoli, Thermoluminescence (TL) characterization of the perovskite-like KMgF 3, activated by Lu impurity, J. Mater. Sci. 39 (2004) 1601–1607. doi:10.1023/B:JMSC.0000016158.40738.d1.

[41] C. Dotzler, G.V.M. Williams, U. Rieser, J. Robinson, Photoluminescence, optically stimulated luminescence, and thermoluminescence study of RbMgF3: Eu2+, J. Appl. Phys. 105 (2009) 1–8. doi:10.1063/1.3068355.

[42] A.J.J. Bos, N.R.J. Poolton, J. Wallinga, A. Bessire, P. Dorenbos, Energy levels in YPO4:Ce3+,Sm3+ studied by thermally and optically stimulated luminescence, Radiat. Meas. 45 (2010) 343–346. doi:10.1016/j.radmeas.2010.01.014.